# Lattice simulations of 2-colour QCD with Wilson fermions

Jon-Ivar SKULLERUD[1,2,*)], Shinji EJIRI[3], Simon HANDS[4] and Luigi SCORZATO[5,6]

[1] *ITF, Universiteit van Amsterdam, Valckenierstraat 65, 1018 XE Amsterdam, The Netherlands*
[2] *School of Mathematics, Trinity College, Dublin 2, Ireland*
[3] *Fakultät für Physik, Universität Bielefeld, Universitätsstraße 25, 33615 Bielefeld, Germany*
[4] *Department of Physics, University of Wales Swansea, Singleton Park, Swansea SA2 8PP, Wales*
[5] *Theory Group, DESY, Notkestraße 85, 22603 Hamburg, Germany*
[6] *Institut für Physik, Humboldt Universität zu Berlin, 12489 Berlin, Germany*

We report on the status of our simulations of two-colour QCD with two flavours of Wilson quarks, at nonzero chemical potential and diquark source. Preliminary results are presented for the static quark potential, gluon propagator, and meson and diquark spectrum.

## §1. Motivation

QCD at non-zero density is currently an area of great activity, as the wide range of presentations at this workshop bears witness. What is missing at present, however, is a first-principles, nonperturbative approach to QCD at high density and low temperature, without which we have little hope of obtaining quantitative predictions regarding the expected complex phase structure in this regime. Lattice QCD would be the natural candidate for such an approach, but it is severely hampered by the fact that the euclidean action becomes complex when a non-zero chemical potential is introduced. Ref. 1) gives an overview of lattice QCD at non-zero density and the problems encountered.

We may avoid these problems by studying model theories which share some of the salient features of QCD, while having a positive definite fermion determinant also for non-zero chemical potential. Examples of such theories are 2-colour QCD,[2)] QCD with adjoint fermions,[3)] NJL models,[4),5)] and QCD with isospin chemical potential.[6)] Here we will be concentrating on 2-colour QCD, which in the gauge sector is expected to be very similar to real QCD, although the baryon sector and chiral properties of the two theories are radically different.

It is of fundamental importance that a theory to be studied using lattice regularisation have a well-defined continuum limit. In the context of non-abelian gauge theories, this implies that the theory should exhibit asymptotic freedom. For SU(2) the second term in the perturbative $\beta$-function changes sign for $N_f \geq 5.6$, with radical consequences for the infrared behaviour of the theory; nonperturbative effects reducing this critical value of $N_f$ still further cannot be ruled out. Consequently we prefer to work with $N_f = 2$ so that both asymptotic freedom (and hence a

*) Talk by Jon-Ivar Skullerud

continuum limit) and confining behaviour in the infrared are guaranteed. Most simulations up to now have been performed using staggered fermions, where either $N_f$ is a multiple of 4, or a square-root of the fermion determinant is taken, making the action non-local. To avoid the potential pitfalls this creates we are here using the Wilson action with $N_f = 2$ quark flavours. This action has also been employed by the Hiroshima group,[7),8)] albeit with a different gauge action, so our results may be directly compared to theirs.

It is also worth pointing out that for $\kappa = \kappa_c$ Wilson fermions, unlike staggered fermions, have the same global symmetry properties as continuum 2-color QCD, as encoded by the Dyson index $\beta = 1$,[3)] which has consequences for the physical spectrum of the model as analysed in Ref. 9).

We now list some physical motivations for studying this model.

### 1.1. *Phase diagram*

There are indications, from studies at nonzero isospin-chemical potential, that the curvature of the phase transition line in the $(T, \mu)$-plane for low $\mu$ is the same as in real QCD. If this can be confirmed, we may gain insight into the phase diagram of real QCD by studying 2-colour QCD, where numerical studies are not restricted to small $\mu/T$.

At the other end of the phase diagram, at low $T$ and high $\mu$, a possible tricritical point has been identified.[10)] A confirmation of this would be welcome. Another interesting issue at low $T$ and intermediate $\mu$ is whether 2-colour QCD has a normal matter phase, i.e. a phase with nonzero baryon number density and zero diquark condensate — or whether the finite-$\mu$ transition is directly from the vacuum to a superfluid phase. The available evidence, as well as chiral perturbation theory studies, indicate the latter, but the matter has not yet been finally settled.

### 1.2. *Spectrum*

Previous studies of 2-colour QCD with Wilson fermions[7),8)] have indicated that the vector meson becomes lighter with increasing chemical potential, in line with the predictions of Brown–Rho scaling[11)] which have been put forward as a possible explanation for the CERES results.[12)] Such an in-medium effect, if confirmed, would provide a new testing ground in heavy-ion experiments such as the one planned at GSI. Closely related to in-medium modification of vector meson properties is the possibility of vector condensation, which may occur instead of or in addition to scalar diquark condensation at high density.[13),14)]

The behaviour of the pseudoscalar isosinglet diquark at high density is also of interest, since it shares the quantum numbers of the $\eta'$ meson but is accessible via standard lattice spectroscopic techniques. Its becoming light as $\mu$ increases may signal the restoration of $\mathrm{U}(1)_A$ symmetry in dense matter.[15)]

Finally, we hope to compare the actual behaviour of the pion and the C-even and -odd scalar diquark masses, as well as the baryon density and chiral and diquark condensates, with the predictions from chiral perturbation theory.[9)] The agreement (for the chiral condensate in particular) is striking in the staggered adjoint model[16)] which is in the same global symmetry class ($\beta = 1$) as the model we are studying here. At some point, of course, chiral perturbation should cease to be accurate once $\mu$ becomes comparable with the mass of the vector diquark, and it is important to know the range of parameters where this breakdown can be anticipated.

### 1.3. *Gluodynamics*

Gluodynamics is arguably the sector where results from two-colour QCD have most direct relevance to real QCD. At zero chemical potential, the gluodynamics of SU(2) and SU(3) are so similar that SU(2) simulations have often been used as a 'cheaper' way of obtaining results relevant to QCD. This is also where we most directly can study effects of fermion loops, including Pauli blocking at high density. In contrast, all numerical results for spectrum and condensates to date might conceivably have been obtained in the quenched approximation.

Among the quantities of particular interest are:

- Polyakov line screening and static quark potential. Previous simulations of SU(2) with Wilson fermions have reported signs of a deconfinement transition at large $\mu$,[8] while no such transition has been observed with staggered fermions.
- Gluon propagator. This quantity is an essential ingredient also in the Dyson–Schwinger equation approach to gauge theories.[17,18] These approaches can be applied equally to SU(2) and SU(3) gauge theories, so input from SU(2) lattice simulations may provide a valuable check on the methods and assumptions used.
- Other quantities that may provide further insight into the phase transition include glueball masses[19] and the gluon condensate.[20]

## §2. Algorithm

Above the critical chemical potential $\mu_c$ for diquark condensation, it is essential to have a diquark source. This serves two purposes:

1. It lifts (near-)zero eigenvalues from the Goldstone modes, improving the condition number and avoiding critical slowing down.
2. It also enables the determination of diquark condensates and other anomalous propagation.

The action, including diquark source terms, can be written

$$\begin{aligned} S =&\overline{\psi}_1 M(\mu)\psi_1 + \overline{\psi}_2 M(\mu)\psi_2 \\ &+ j\left[\psi_2^{tr}\tau_2 C\gamma_5\psi_1 - \psi_1^{tr}\tau_2 C\gamma_5\psi_2\right] + \overline{\jmath}\left[\overline{\psi}_2\tau_2 C\gamma_5\overline{\psi}_1^{tr} - \overline{\psi}_1\tau_2 C\gamma_5\overline{\psi}_2^{tr}\right], \end{aligned} \tag{2·1}$$

where $j, \overline{\jmath}$ are sources for the diquark and antidiquark respectively, and $M(\mu)$ is the usual Wilson-fermion matrix. If we introduce $\widetilde{M}(\mu) \equiv \gamma_5 M(\mu)$ and the new field variables

$$\chi_1 = \psi_1\,, \qquad \overline{\chi}_1 = \overline{\psi}\gamma_5\,, \qquad \phi_2^{tr} = \psi_2^{tr}\tau_2 C\gamma_5\,, \qquad \overline{\phi}_2^{tr} = \tau_2 C\overline{\psi}_2^{tr}\,, \tag{2·2}$$

the action can be rewritten as

$$S = \begin{pmatrix}\phi_2^{tr} & \overline{\chi}_1\end{pmatrix} \begin{pmatrix} j & \widetilde{M}(\mu) \\ \widetilde{M}(-\mu) & -\overline{\jmath}\end{pmatrix} \begin{pmatrix}\chi_1 \\ \overline{\phi}_2^{tr}\end{pmatrix} \equiv \overline{X} Q[\mu, j, \overline{\jmath}] X\,. \tag{2·3}$$

The matrix $Q$ is hermitean, and the determinant is negative definite if the two sources are equal: $j = \bar{\jmath}$, so this representation lends itself to simulation using standard algorithms.

We will use the two-step multibosonic algorithm,[21] which has been shown to be more efficient than Hybrid Monte Carlo (HMC) in the dense phase,[3] and which is ergodic even in the presence of singularities. However, in the initial phase, we have also performed simulations using HMC without a diquark source, and these are the results we will quote in the following.

## §3. Results

In order to establish a baseline, we have first performed simulations on $8^3 \times 16$ lattices at $\mu = 0$, for several values of $\beta$ and $\kappa$, using the standard Wilson action both for gauge fields and for fermions. The parameters are given in table I, along with the associated average spatial and timelike plaquette values. We have sampled configurations every 4 trajectories.

| $\beta$ | $\kappa$ | $dt$ | $N_{\rm traj}$ | acc | $\Box_s$ | $\Box_t$ | Name |
|---|---|---|---|---|---|---|---|
| 1.7 | 0.1780 | 0.0125 | 7152 | 84% | 0.47386(6) | 0.47367(6) | coarse (c) |
| 1.8 | 0.1725 | 0.02 | 3856 | 70% | 0.50007(8) | 0.49983(8) | |
| | 0.1740 | 0.01 | 216 | 89% | | | |
| | | 0.0125 | 272 | 80% | 0.5056(2) | 0.5052(2) | |
| | 0.1750 | 0.01 | 600 | 80% | 0.5140(3) | 0.5139(3) | light (l) |
| 1.9 | 0.1650 | 0.02 | 2316 | 83% | 0.52124(10) | 0.52098(10) | fine (f) |

Table I. Hybrid Monte Carlo simulation parameters, $\mu = 0$. $dt$ is the HMC timestep, while 'acc' denotes the acceptance rate. $\Box_s$ and $\Box_t$ are the average spatial and timelike plaquette values respectively.

### 3.1. *Setting the scale*

We have attempted to set the scale from the string tension by computing Creutz ratios. Figure 1 shows the results for the coarse lattice ($\beta = 1.8, \kappa = 0.178$) which is where we have the best statistics. It is evident from the figure that our statistics are still not sufficient to determine the string tension from Creutz ratios with any degree of confidence, and from the other parameter values the situation is even worse. Based on the trend displayed by the data, we tentatively estimate $a^2\sigma \approx 0.37(5)$. Taking the string tension to be $\sqrt{\sigma} \approx 420$ MeV, this gives a lattice spacing $a \approx 0.29$ fm or $a^{-1} \approx 690$ MeV.

In Fig. 2 we show Creutz ratios for $R = 2$ only for all our parameter values. We also include the $R = 3, 4$ data for the light lattice ($\beta = 1.8, \kappa = 0.175$), to give an indication of the trend. We may attempt to determine ratios of lattice spacing by simply taking the ratios of Creutz ratios at $(R = 2, T = 3)$ where the statistics permit this. The results are shown in table II. These numbers are likely to be overestimates, since ratios for $R = 2$ appear to increase rather than decrease with $T$.

We have also attempted to determine the lattice spacing ratios by matching

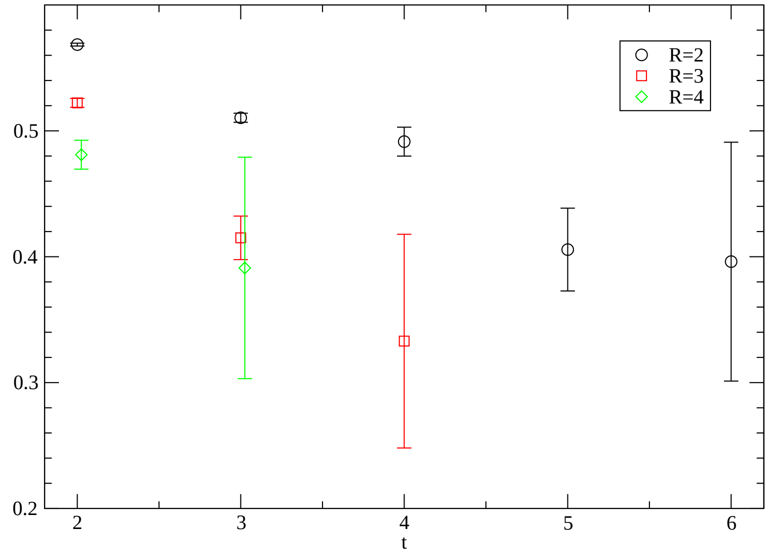


Fig. 1. Creutz ratios for the coarse lattice ($\beta = 1.7, \kappa = 0.178$).

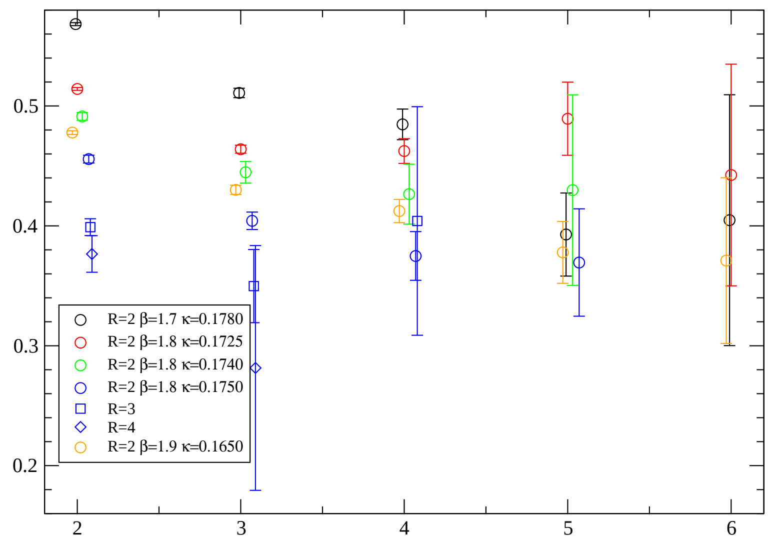


Fig. 2. Creutz ratios for $R = 2$, all $(\beta, \kappa)$ values.

| | | Creutz | Gluon | | |
|---|---|---|---|---|---|
| $\beta$ | $\kappa$ | $R_a$ | $R_a$ | $R_Z$ | $\chi^2/N_{df}$ |
| 1.7 | 0.1780 | 1 | 1 | 1 | — |
| 1.8 | 0.1725 | 0.95 | 0.84(1) | 1.06 | 9.7 |
| | 0.1740 | 0.93 | 0.76(2) | 1.06 | 2.0 |
| | 0.1750 | 0.89 | 0.69(3) | 1.06 | 2.7 |
| 1.9 | 0.1650 | 0.92 | 0.74(1) | 1.14 | 20 |

Table II. Ratios of lattice spacings $R_a = a/a_c$, where $a_c$ is the lattice spacing on the coarse lattice. 'Creutz' denotes the ratios of Creutz ratios for $R = 2, T = 3$, while 'Gluon' denotes the outcome of matching the gluon propagator as described in Ref. 22), with $R_Z$ being the ratio of renormalisation constants $Z_3/Z_3^c$.

the (Landau-gauge) gluon propagator as described in Ref. 22). We have imposed a cylinder cut, selecting points within a radius $1.2 \times \pi/8a$ from the diagonal in momentum space, and varied the ratios of lattice spacing $a$ and gluon renormalisation constant $Z_3$ to match the gluon propagator for the different parameters. In Fig. 3 we show the gluon form factor before and after matching. The resulting $a$ and $Z_3$ ratios are given in table II.

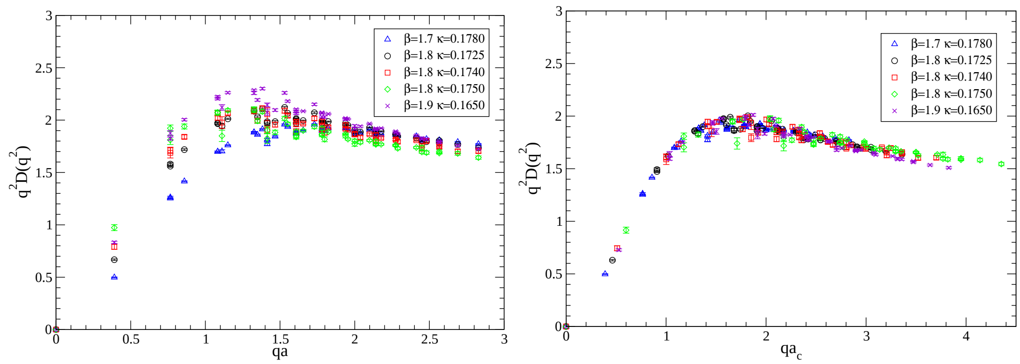


Fig. 3. The gluon propagator form factor in Landau gauge, as a function of momentum. Left: before matching of lattice spacings; right: after matching.

This procedure should be treated with some caution, since it can fail on three counts. Firstly, in the presence of dynamical fermions the renormalised gluon propagator will depend on the renormalised fermion masses, which vary between our parameter sets. This may explain the discrepancy between the data for ($\beta = 1.8, \kappa = 0.175$) and ($\beta = 1.9, \kappa = 0.165$) at large momenta since, as we shall see, these two have the lightest and the heaviest quark mass respectively. Secondly, on these coarse lattices it is likely that we are not in the scaling regime so the renormalised propagator will have a substantial cutoff dependence. Thirdly, since the volume is fixed in lattice units, these lattices will have different physical volumes and finite volume effects should cause a slight mismatch in the infrared, where our procedure has left them almost perfectly matched. In particular, for the lightest quark mass, corresponding to the finest lattice, we see quite large lattice artefacts at intermediate momenta, which may arise from finite volume effects. For the other lattices however, the physical volumes are so large that such effects are likely to be quite small.

With these caveats in mind, the two methods may complement each other and give an idea of the systematic uncertainties in the lattice spacings. It would clearly be preferable to compute the static quark potential using smeared Wilson loops, but even this may fail to provide a reliable lattice spacing on these small lattices.

### 3.2. *Meson and diquark spectrum*

We have computed correlators, using point sources, for the pseudoscalar ($\pi$), scalar ($\delta$) and vector ($\rho$) mesons, as well as for the scalar, pseudoscalar and vector diquarks. For the vector diquark we have not been able to extract a mass, while the scalar and pseudoscalar diquarks are exactly degenerate with the $\pi$ and $\delta$, as they should be at $\mu = 0$. In the following, we will therefore only quote our results for the meson spectrum, with the main quantity of interest being $m_\pi/m_\rho$.

In Figure 4 we show the effective meson masses for ($\beta = 1.7, \kappa = 0.178$). We see, firstly, that with point sources on these lattices, we do not get a good plateau for either of these correlators, and secondly, that the $\delta$ correlator is still too noisy to determine the mass with any confidence, although clearly $m_\delta \gg m_\pi$, implying we are in a phase where chiral symmetry is spontaneously broken. Although we do not see a plateau, we can still fit the $\pi$ and $\rho$ correlators to a double-exponential (cosh) with a good to reasonable $\chi^2$. The resulting masses are given in table III. However, as the absence of a plateau in the effective-mass plot would indicate, the fit values are not stable, and one should add a systematic uncertainty of 1–2% in all quantities from the variation with the fit range.

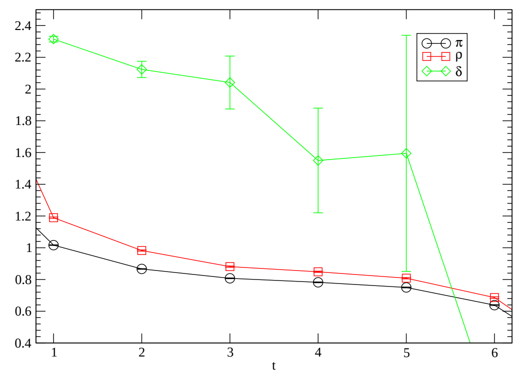


Fig. 4. Effective masses for ($\beta = 0.17, \kappa = 0.178$).

| $\beta$ | $\kappa$ | $m_\pi$ | $\chi^2/N_{df}$ | $m_\rho$ | $\chi^2/N_{df}$ | range | $m_\pi/m_\rho$ |
|---|---|---|---|---|---|---|---|
| 1.7 | 0.1780 | 0.800(2) | 0.97 | 0.870(3) | 1.4 | 3–5 | 0.920(3) |
| 1.8 | 0.1725 | 0.807(3) | 1.3 | 0.859(4) | 0.82 | 4–6 | 0.939(4) |
| | 0.1740 | 0.731(9) | 2.5 | 0.820(14) | 1.6 | 3–5 | 0.892(15) |
| | 0.1750 | 0.642(9) | 0.64 | 0.726(15) | 1.4 | 3–5 | 0.885(16) |
| 1.9 | 0.1650 | 0.925(4) | 0.27 | 0.973(5) | 0.12 | 4–6 | 0.951(4) |

Table III. Meson masses. $m_\pi$ and $m_\rho$ are obtained by fitting the correlators to a cosh function on the timeslices denoted by 'range' (and their mirror images around the centre of the lattice). The errors are purely statistical bootstrap errors.

Comparing tables II and III it appears that the lattice spacing changes somewhat more rapidly with $\kappa$ at fixed $\beta$ than the $\pi$-to-$\rho$ mass ratio. A more careful analysis is needed to identify the true lattice spacing and spectrum before it can be determined whether this is a real effect or merely a sign of shortcomings in our analysis.

Finally, in Fig. 5 we show the scalar meson and vector diquark correlators as a function of time. Both correlators change sign, so we plot the absolute value in order to show them on a logarithmic scale.

## §4. Outlook

We have performed initial simulations to explore the parameter space for 2-colour QCD with Wilson fermions. The next step will be to extend the simulations at one or more of these points to non-zero chemical potential. Preliminary studies show that HMC experiences a dramatic slowing-down as we approach the expected transition point at $\mu = m_\pi/2$. We will therefore be using the TSMB algorithm to explore densities beyond this point.

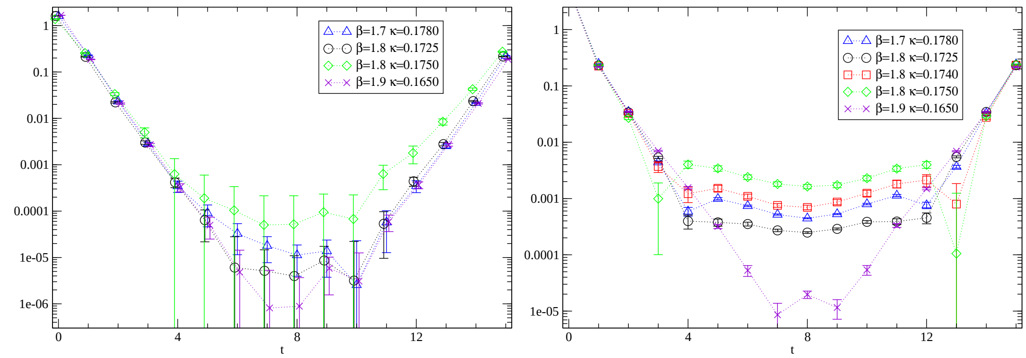


Fig. 5. Absolute value of the scalar meson (left) and vector diquark (right) correlators.

## Acknowledgements

JIS acknowledges support from FOM/NWO. SJH is supported by a PPARC Senior Research Fellowship.

### References

1) S. Muroya, A. Nakamura, C. Nonaka and T. Takaishi, Prog. Theor. Phys. **110** (2003), 615 [hep-lat/0306031].
2) S. Hands, J. B. Kogut, M.-P. Lombardo and S. E. Morrison, Nucl. Phys. **B558** (1999), 327 [hep-lat/9902034].
3) S. Hands *et al.*, Eur. Phys. J. **C17** (2000), 285 [hep-lat/0006018].
4) S. Hands and D. N. Walters, Phys. Lett. **B548** (2002), 196 [hep-lat/0209140].
5) D. N. Walters, hep-lat/0310038, this volume.
6) J. B. Kogut and D. K. Sinclair, Phys. Rev. **D66** (2002), 034505 [hep-lat/0202028].
7) S. Muroya, A. Nakamura and C. Nonaka, Phys. Lett. **B551** (2003), 305 [hep-lat/0211010].
8) S. Muroya, Color SU(2) lattice QCD high density state, this volume.
9) J. Kogut, M. Stephanov, D. Toublan, J. Verbaarschot and A. Zhitnitsky, Nucl. Phys. **B582** (2000), 477 [hep-ph/0001171].
10) J. B. Kogut, D. Toublan and D. K. Sinclair, Nucl. Phys. **B642** (2002), 181 [hep-lat/0205019].
11) G. E. Brown and M. Rho, Phys. Rev. Lett. **66** (1991), 2720.
12) CERES/NA45, G. Agakishiev *et al.*, Phys. Lett. **B422** (1998), 405 [nucl-ex/9712008].
13) K. Langfeld, H. Reinhardt and M. Rho, Nucl. Phys. **A622** (1997), 620 [hep-ph/9703342].
14) F. Sannino and W. Schäfer, Phys. Lett. **B527** (2002), 142 [hep-ph/0111098].
15) T. Schäfer, Phys. Rev. **D67** (2003), 074502 [hep-lat/0211035].
16) S. Hands, I. Montvay, L. Scorzato and J. Skullerud, Eur. Phys. J. **C22** (2001), 451 [hep-lat/0109029].
17) C. D. Roberts and S. M. Schmidt, Prog. Part. Nucl. Phys. **45S1** (2000), 1 [nucl-th/0005064].
18) R. Alkofer and L. von Smekal, Phys. Rept. **353** (2001), 281 [hep-ph/0007355].
19) M. P. Lombardo, M. L. Paciello, S. Petrarca and B. Taglienti, hep-lat/0309110.
20) M. Baldo, P. Castorina and D. Zappalà, nucl-th/0311038.
21) I. Montvay, Nucl. Phys. **B466** (1996), 259 [hep-lat/9510042].
22) UKQCD, D. B. Leinweber, J. I. Skullerud, A. G. Williams and C. Parrinello, Phys. Rev. **D60** (1999), 094507 [hep-lat/9811027].